Electronic Supplementary Material (ESI) for RSC Advances

Electronic supplementary information

Pareto-optimal Transparent Conducting Oxides

Redouane MILOUA, Zoubir KEBBAB, Noureddine BENRAMDANE

Laboratoire d'Elaboration et Caractérisation des Matériaux
P.O. BOX 89, Faculty of Engineering Sciences,
Djillali Liabes University of Sidi Bel-Abbes, 22000 Algeria

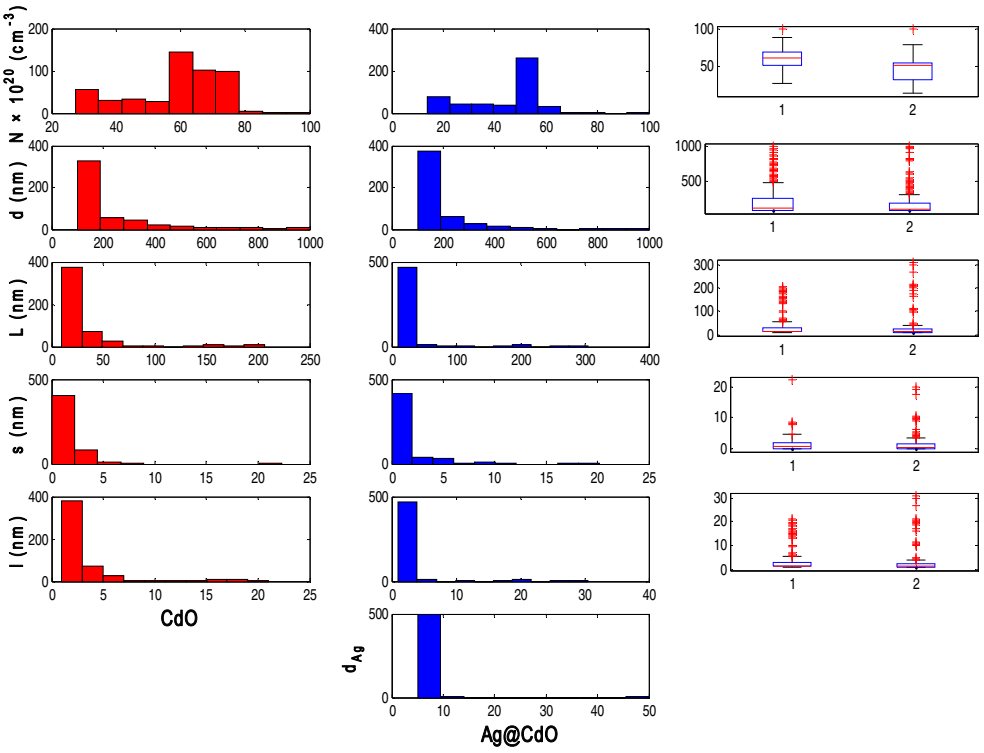

Figure S1: Histograms and box plots for variable distributions of CdO (1) and Ag@CdO (2).

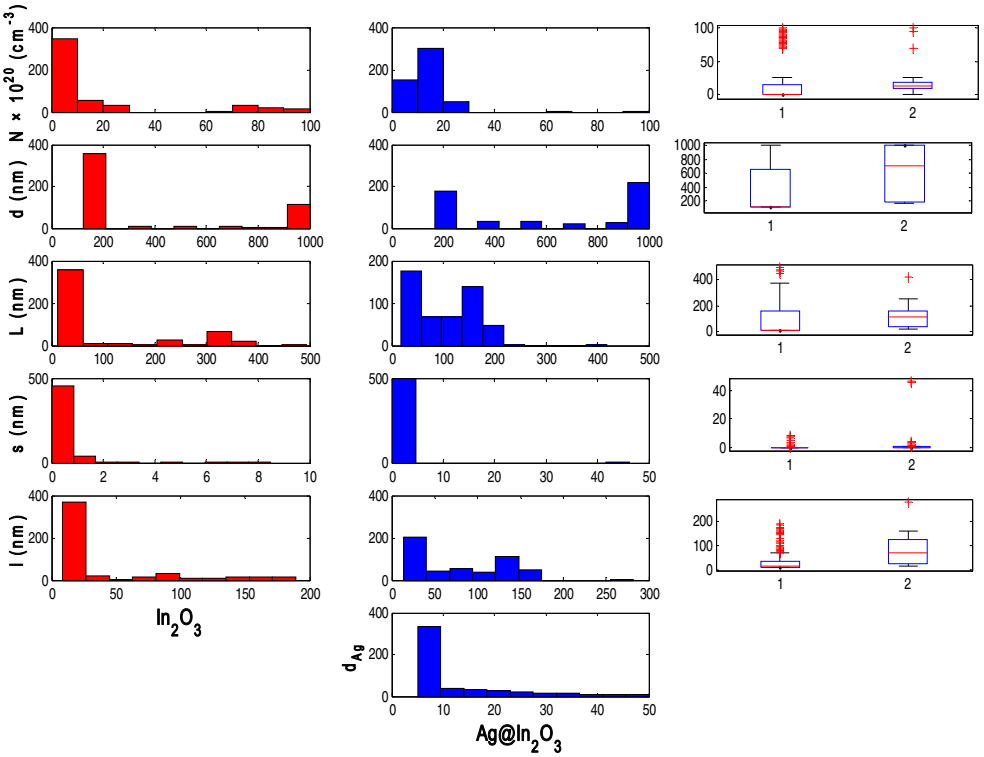

Figure S2: Histograms and box plots for variable distributions of In_2O_3 (1) and Ag@In_2O_3 (2).

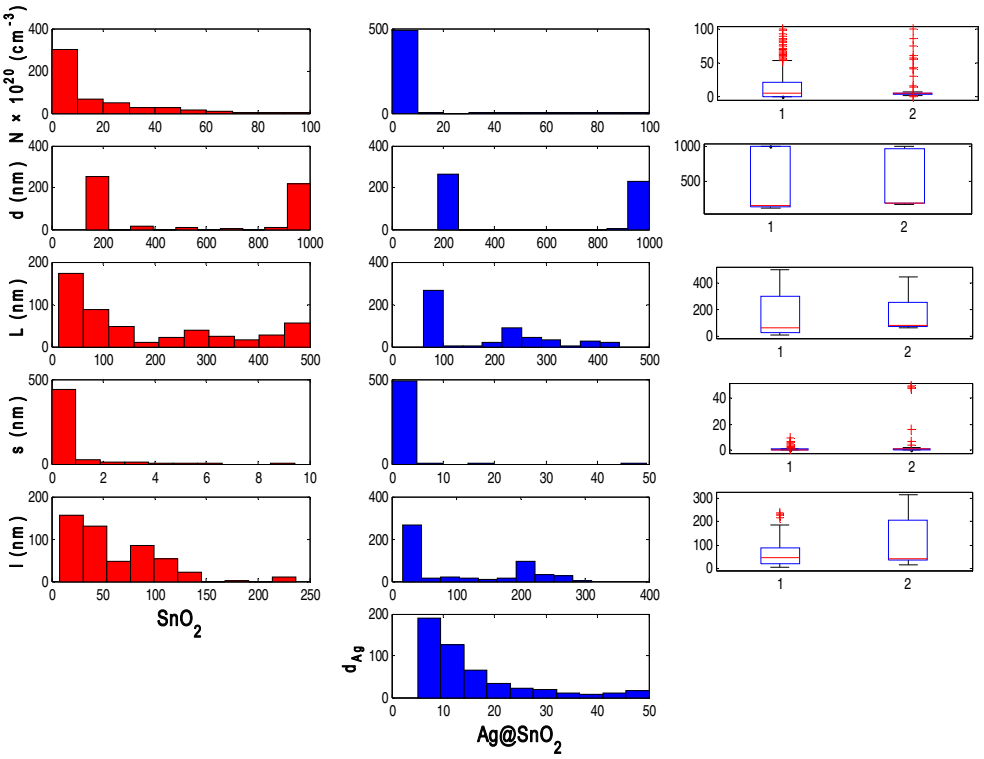

Figure S3: Histograms and box plots for variable distributions of SnO_2 (1) and Ag@SnO_2 (2).

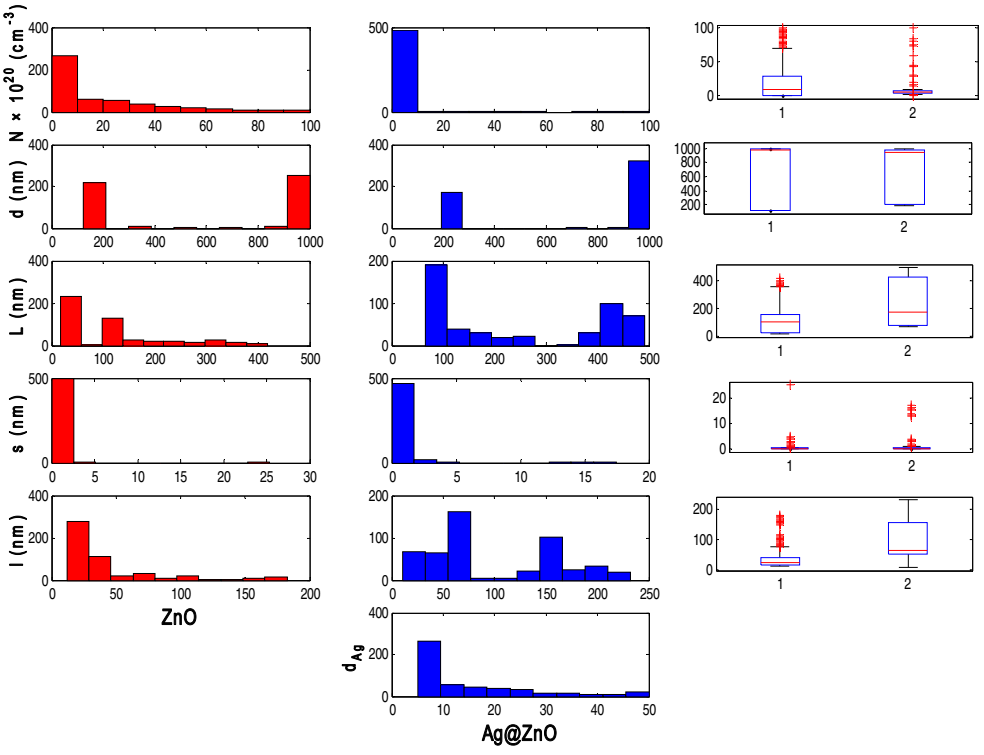

Figure S4: Histograms and box plots for variable distributions of ZnO (1) and Ag@ZnO (2).

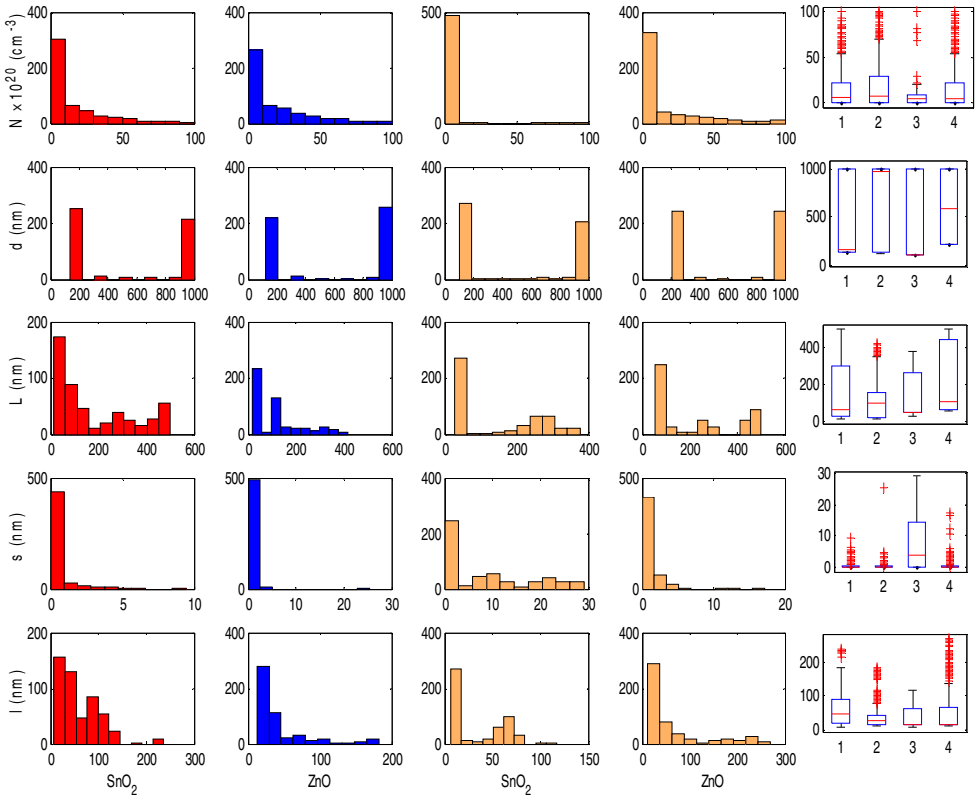

Figure S5: Histograms and box plots for variable distributions of SnO_2 (1), ZnO (2) and SnO_2/ZnO (3/4).

Construction of the TCO numerical model:

The model is constructed by using TCO transport equations[1-4] combined to the optical matrix method[5,6] to calculate both optical response and sheet resistance of a multilayer system. For each TCO layer, the model requires five input variables which are constrained by the following inequalities:

$$10^{19} \leq N \leq 10^{21}$$
$$100 \leq d \leq 1000$$
$$0 \leq \rho \leq 50$$
$$10 \leq L \leq 0.5 \times d$$
$$1 \leq \ell \leq 0.9 \times L$$
$$5 \leq d_{Ag} \leq 50$$

In Ag@TCO systems, the Ag layer is characterized by its thickness d_{Ag} (nm). The effect of carrier concentration on the optical transmittance is obtained by associating a Drude term to the dielectric function of undoped TCO as described elsewhere[7]. In multilayer systems, the equivalent sheet resistance $R_{\square}^{eq}$ is obtained from sheet resistances of each layer $R_{\square}^{k}$ as $\frac{1}{R_{\square}^{eq}} = \sum_{k} \frac{1}{R_{\square}^{k}}$. All materials constants (i.e. optical constants, effective masses, trap densities, etc.) were retrieved from the literature[7-10]. The optical constants of CdO were obtained from fitting of transmittance data of a spray pyrolysed CdO layers. Moreover, transport phenomena in CdO are treated following indications from Ref. 4.

Calculation of the short-circuit current and the conversion efficiency:

The maximum photocurrent I_{ph} is obtained by integrating the transmittance multiplied by the AM1.5G solar spectrum, over the range of 280 nm to $\lambda_g = \frac{1240}{E_g}$. We choose Eg = 1.5 eV which is typically the band gap of CdTe. The short circuit current and conversion efficiency are calculated for each point of the Pareto-optimal set using the single diode equivalent scheme including series and shunt resistances, R_s and R_{sh} respectively. For the sake of simplicity, we assume $R_s = R_{sheet} \times L^2/3$ (L = 1cm) and $R_{sh} = \infty$. The ideality factor is taken as n = 1, the saturation current I_{sat} is estimated from the empirical formula by Green et al.[11].

References:

1. Seto, J. Y. The electrical properties of polycrystalline silicon films. *J. Appl. Phys.* **46** 5247-5254 (1975).
2. Steinhauser, J. et al. Transition between grain boundary and intragrain scattering transport mechanisms in boron-doped zinc oxide thin films. *Appl. Phys. Lett.* **90** 142107-142109 (2007).
3. Ellmer, K., Klein, A. & Rech, B. *Transparent conductive zinc oxide, basics and applications in thin film solar cells* (Springer, Berlin, 2008).
4. Vasheghani Farahani, S. K. et al. Electron Mobility in CdO Films. *J. Appl. Phys.* **109**, 073712-073716 (2011).
5. Singh, J. *Optical properties of condensed matter and applications* (John Wiley & Sons Ltd, England, 2006).

6. Carniglia, C. K. Scalar scattering theory for multilayer optical coatings. *Opt. Eng.* **18**, 104-115 (1979).
7. Lai, F. et al. Determination of optical constants and thicknesses of In_2O_3:Sn films from transmittance data. *Thin Solid Films* **515**, 7387-7392 (2007).
8. Miao, L. et al. Spectroscopic ellipsometry study of In_2O_3 thin films. *J. Mater. Sci: Mater Electron* **20**, 71-75 (2009).
9. Von Rottkay, K. & Rubin, M. Optical indices of pyrolytic tin-oxide glass. *Mater. Res. Soc. Symp. Proc.* **426**, 449-455 (1996).
10. Liu, Y. C., Hsieh, J. H. & Tung, S. K. Extraction of optical constants of zinc oxide thin films by ellipsometry with various models. *Thin Solid Films* **510**, 32-38 (2006).
11. Markvart, T. & Castaner, L. *Solar cells: materials, manufacture and operation*, (Elsevier, Oxford, 2004), see p. 63.

The Pareto optimality:

The Pareto optimality is a concept from economics with applications in engineering, social science and recently in materials science [1], especially when a problem involves solutions based on multiple and conflicting criteria. In such a problem, it is difficult to assign a metric (or figure of merit) to different objectives. The difficulty is increased by the fact that even small numeric changes in weights can generate very different solutions. Such a situation is encountered in TCO optimal design.

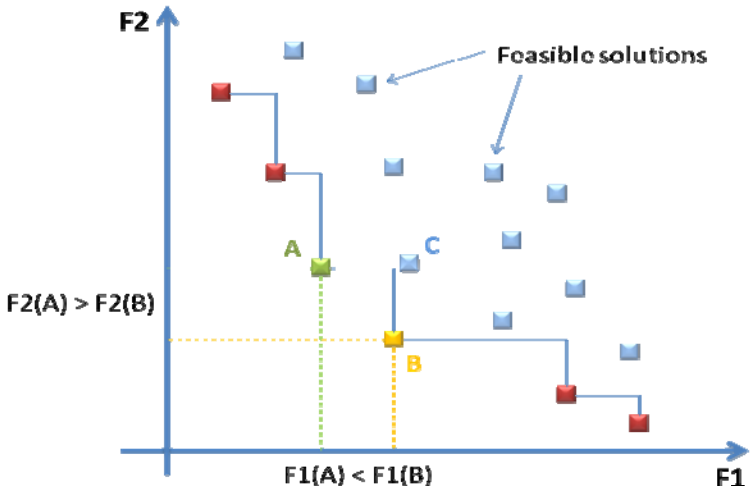

Figure S6: Example of a Pareto front: the boxed points represent feasible solutions, if we want to minimize both F1 and F2 smaller values are preferred to larger ones. Point *C* is not on the Pareto front because it is dominated by both point *A* and point *B*. Points *A* and *B* are not strictly dominated by any other, and hence do lie on the front.

Usually, choosing a good TCO material for a certain application involves the use of a figure-of-merit (FOM) relating the optical transparency and the electrical conductivity (or resistivity) in a simple manner, e.g. the Haacke's FOM [2]:

$$\phi_{TC} = \frac{T^{10}}{R_{sheet}}$$

This FOM suffers from the following drawbacks:

- Since T and R_{sheet} are inversely proportional, it is possible to have the same value of ϕ_{TC} for totally different TCO coatings.
- The weighting has no physical justification.
- Recent works demonstrate that with the increase of transparency of new materials (carbon nanotubes), this model became no longer valid [3].
- The model is not correlated to the device performance [4].

What makes our approach better is that we avoid all these drawbacks and hence gain in generality and accuracy. Our approach models real TCO systems by a correct theoretical

model [5], and then explores all feasible input values of the model and extracts those which satisfy the Pareto optimality, i.e. minimizing both optical loss and sheet resistance. After that, data clustering is used to screen potential Pareto solutions which are suitable for an a priori chosen application (see the flowchart in Fig.1).

[1] T. Bligaard et al., *Appl. Phys. Lett.,* 2003, **83**, 4527. [2] G. Haacke, *J. Appl. Phys*., 1976, **47**, 4086. [3] Á. Pekker, and K. Kamarás, *J. Appl. Phys.,* 2010, **108**, 054318. [4] X. Huang et al., *J. Renewable Sustainable Energy*, 2009, **1**, 063107. [5] S. Faÿ et al., Thin Solid Films, 2010, **518**, 2961.

Correlation to experimental works:

Table TS1: Transparency and sheet resistance of some TCO structures.

TCOs	Transparency (%)	R_{sheet} (Ohms/sq)	Refs
CdO	79.5	5	[1]
	86.4	5	[4]
In_2O_3	85.3	10.8	[1]
	92.3	10.5	[4]
	85	27	[6]
	92	11	[6]
	85	62	[7]
	80	6.74	[8]
	85	9.34	[9]
	90	12	[6]
SnO_2	46.2	2	[14]
	64.3	4	[14]
	67.1	10	[14]
	82.7	15	[14]
	75	4	[15]
	85	8.1	[16]
ZnO	80	10	[10]
	85	4.6	[11]
	90	4	[13]
Ag@In_2O_3	87	6.3	[2]
Ag@ZnO	92.5	4.2	[3]
	78	8.5	[12]
	77.5	6.5	[12]
	74	5.2	[12]
	71	14	[12]
	80.5	6.5	[12]
	78	5.5	[12]
	72	6	[12]
	76.5	7	[12]
	77.5	6.5	[12]
	74	6.8	[12]
CdO/In_2O_3	79.7	4.9	[1]
	87.6	5	[4]
	86.8	4.9	[4]
In_2O_3/ZnO	80	32	[5]

References:

[1] J. Liu et al., Chem. of Mater., 2008, **21**, 5258. [2] L. Zhang et al., Proc. of SPIE, 2007, **6722**, 67222Q. [3] J. Yan et al., Proc. of SPIE, 2008 , **6624**, 662413. [4] J. Liu et al., Thin Solid Films, 2010, **518**, 3694. [5] C.-C Liu et al., Sol. Ene. Mater. Sol. Cells, 2009, **93**, 267. [6] H. Kim et al., J. Appl. Phys., 1999, **86**, 6451. [7] W.-F. Wu et al., Semicond. Sci. Technol., 1994, **9**, 1242. [8] C. W. Tang and S. A. Van Slyke, Appl. Phys. Lett., 1987, **51**, 913. [9] P. Nath et al., Thin Solid Film, 1980, **72**, 463. [10] Xin-liang Che et al., Thin Solid Films, 2011, **520**, 1263. [11] Xuhu Yu et al., Journal of Crystal Growth 2005, **274**, 474. [12] A. El Hajj et al., Thin Solid Films, 2011, doi:10.1016/j.tsf.2011.10.193. [13] Xuhu Yu et al., Applied Surface Science, 2005, **239**, 222. [14] S.I.

Noh, et al., Ceram. Int., 2012, doi:10.1016/j.ceramint.2012.01.018. [15] D. Miao et al., Journal of Non-Crystalline Solids, 2010, **356**, 2557. [16] P. Veluchamy, Solar Energy Materials & Solar Cells, 2001, **67**, 179.

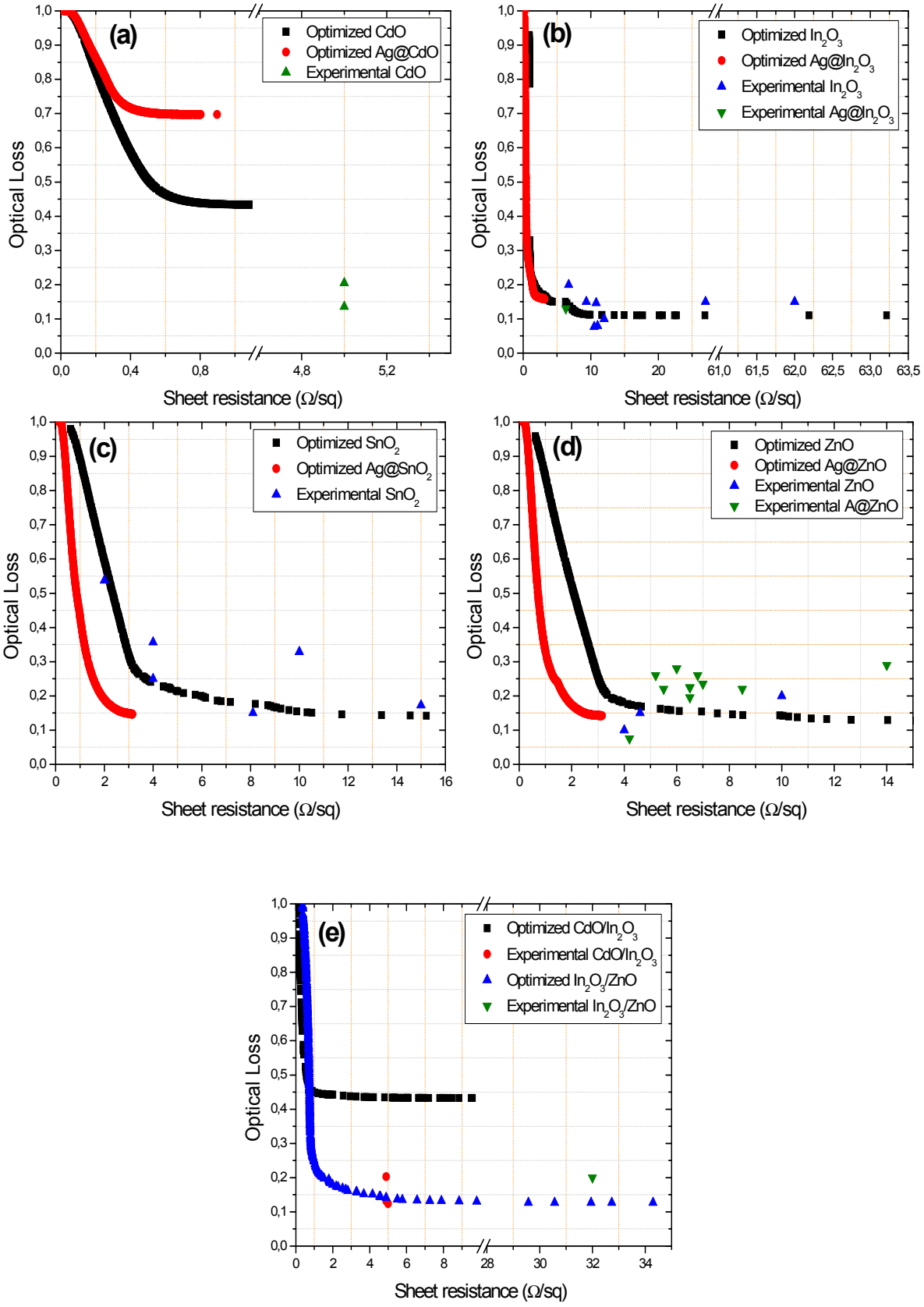

Figure S7 : Optimized vs. experimental optical looses and sheet resistances of some TCO structures: (a) ZnO and Ag@ZnO, (b) In_2O_3 and Ag@In_2O_3, (c) CdO and Ag@CdO, (d) SnO_2 and Ag@SnO_2, (e) CdO/In_2O_3 and In_2O_3/ZnO.

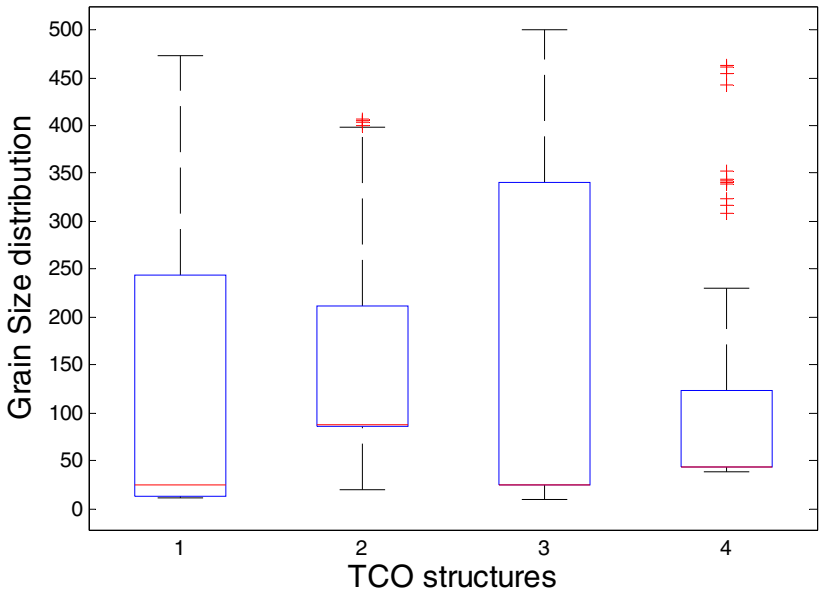

Figure S8: Box plot of grain size distributions of In_2O_3(1), ZnO(2), In_2O_3(3)/ZnO(4) systems.

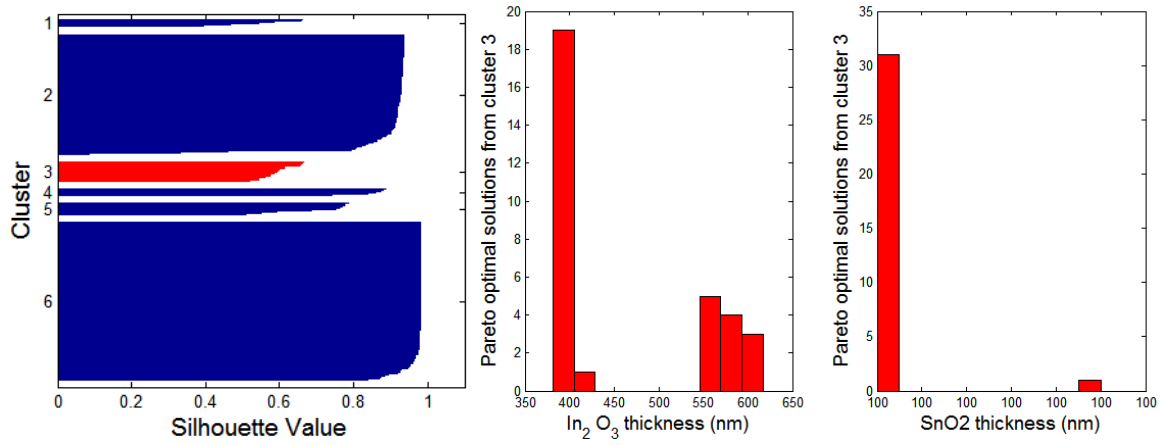

Figure S9: Optimization of the In_2O_3/SnO_2 structure. **Left panel**: Silhouette plot of the Pareto optimal solutions obtained for the In_2O_3/SnO_2 system. The subset of solutions corresponding to cluster #3 is the best in term of conversion efficiency (mean conversion efficiency equal to 22.5 %). **Right panel**: Histograms of In_2O_3 and SnO_2 thicknesses as identified from cluster #3. Most thickness values are located at 375 nm for In_2O_3 and 100 nm for SnO_2.

Figure S7 depicts the calculated Pareto fronts with experimental data from Table TS1 for some TCO systems. For CdO based structures (Fig. S7a, S7e) it is clear that the experimental values exhibit better optical performance than the optimized ones. This is certainly due to the poor optical quality of the CdO films, used in our calculations (the mean transmittance T_m where equal to 46 %). From this we conclude that the calculated results are strongly correlated to the materials properties and by this we can make a correct judgment on the

material's performance. The same behavior is observed for some experimental values depicted in Fig S7b, S7c and S7d. It is straightforward to see that most of the calculated values remain better than the experimental ones in term of the electrical performance. We expect this to be the result of low electron mobility due to the relatively small grain sizes.

From Figure S8 we notice a shift of the In_2O_3(3) grain size distribution resulting in the enhancement of the electrical properties of the In_2O_3/ZnO structure. This result is in agreement with the experiments after J. Herrero and C. Guillen, *Thin Solid Films,* 2004, **451**, 630 and R. Vinodkuma et al. *Solar Energy Materials & Solar Cells,* 2010, **94**, 68.

For the In_2O_3/SnO_2 system we analyzed the Pareto optimal set with data clustering (Fig. S9). The cluster #3 corresponds to the highest mean conversion efficiency. Thicknesses extracted from the Pareto optimal solutions of cluster #3 ranged from 350 nm to 400 nm for In_2O_3 and at 100 nm for ZnO. This is in excellent agreement with the experimental work after S. Ngamsinlapasathian, (*Solar Energy Materials & Solar Cells,* 2006, **90**, 2129) who suggested that bilayers of 300 nm (ITO) and 100 nm (SnO_2) have the best performance when they are used in dye sensitized solar cells.